Mansoura Engineering Journal

Volume 39 | Issue 1 Article 1

7-15-2020

# Tidal Effect on Groundwater Fluctuations and Saltwater Intrusion in Coastal Heterogeneous Aquifers.

Kassem El-Alfy
*Professor of Hydraulics., Mansoura University, Dean of Mansoura High Institute of Eng. And Technology*, amrorana2003@yahoo.com

Hamdy El-Ghandour
*Assistant prof., Irrigation & Hydraulics Dept., Faculty of Engineering, Mansoura University, Egypt.*, hamdy_elghandour@yahoo.com

Mahmoud Abd-Elmaboud
*M.Sc. Student, Irrigation & Hydraulics Dept., Faculty of Engineering, Mansoura University, Egypt*



Recommended Citation
El-Alfy, Kassem; El-Ghandour, Hamdy; and Abd-Elmaboud, Mahmoud (2020) "Tidal Effect on Groundwater Fluctuations and Saltwater Intrusion in Coastal Heterogeneous Aquifers.," *Mansoura Engineering Journal*: Vol. 39 : Iss. 1 , Article 1.
Available at: https://doi.org/10.21608/bfemu.2020.103086

# Tidal Effect on Groundwater Fluctuations and Saltwater Intrusion in Coastal Heterogeneous Aquifers

# تأثير المد والجزر على تذبذب المياه الجوفية وتداخل المياه المالحة فى الطبقات الجوفية الساحلية الغير متجانسة

Kassem S. El-Alfy [1], Hamdy A. El-Ghandour [2,] Mahmoud E. Abd-Elmaboud [3]
[1] Prof. of Hydraulics, Irrigation & Hydraulics Dept., Faculty of Engineering, Mansoura University, Egypt.
[2] Assistant prof., Irrigation & Hydraulics Dept., Faculty of Engineering, Mansoura University, Egypt.
[3] M.Sc. Student, Irrigation & Hydraulics Dept., Faculty of Engineering, Mansoura University, Egypt.

## خلاصة

يهتم هذا البحث بدراسة تأثير التغير فى منسوب سطح مياه البحر نتيجة أمواج المد و الجزر على كل من تذبذب سطح المياه الجوفية وتداخل المياه المالحة في الطبقات الجوفية الساحلية المحصورة و الغير محصورة. تمت الدراسة علي فرضية وجود سطح فاصل حاد يفصل بين الماء الجوفي المالح والماء العذب. تم بناء نموذج رياضى ثنائى الأبعاد يعتمد على مبدأ فصل حركة المياه الجوفية على المدى الطويل و المدى القصير واستخدمت طريقتي العناصر المحدودة والفروق المحدودة لتمثيل سريان المياه الجوفية وذلك تحت ظروف سريان غير مستقر داخل خزان جوفي محصور مخلق وآخر غير محصور حقيقي غير متجانسين. لعمل نماذج محتملة من التربة الغير متجانسة في الخزان الجوفي المخلق تم إستخدام المعادلة اللوغاريتمية لمعامل النفاذية الحقلية لتوليد قيم مختلفة منه بمعلومية قيمتي المتوسط الحسابي والإنحراف المعيارى، حيث تم تثبيت قيمة المتوسط الحسابي ودراسة تأثير التغير في الإنحراف المعياري. وفي هذا الجزء تم إستنتاج مجموعة من المنحنيات والعلاقات التي توضح مدى إنتشار أمواج المد والجزر داخل الخزان الجوفي خلال الحالات المحتملة من التربة الغير متجانسة وأيضا تأثير ذلك علي حركة السطح الفاصل بين الماء العذب و الماء المالح. وجد أنه كلما زاد قيمة الإنحراف المعيارى قلت مسافة إنتشار أمواج المد والجزر وأيضا يقل معدل تداخل الكتلة المالحة داخل الخزان الجوفي المحصور. إمتدت الدراسة أيضا إلي تطبيق النموذج الرياضى المقترح لتمثيل الخزان الرباعى الساحلى الغير محصور بين رفح ودلتا وادى العريش بشمال سيناء بمصر. في البداية تم بناء الشكل الهندسى لمنطقة الدراسة ثم بناء النظام المائى للخزان بإدخال المعاملات الهيدروليكية المختلفة مثل معاملات النفاذية الهيددروليكية ومعدلات تغذية الخزان الجوفى بالأمطار. تمت معايرة النموذج فى حالة الاتزان بمناسيب المياه المقاسة. وأخيرا تمت دراسة مدي إنتشار أمواج المد و الجزر داخل هذا الخزان الجوفي. وجد أن موجة المد و الجزر يكون إنتشارها أكبر فى منطقة رفح و يقل تدريجيا كلما إتجهنا ناحية وادى العريش لان معمل النفاذية الهيدروليكية يقل تدريجيا من رفح حتى دلتا وادى العريش.

## ABSTRACT

Groundwater table and saltwater wedge in coastal areas are commonly affected by tidal waves fluctuations. In this research, for the first time, a two-dimensional numerical model in plan is developed for simulating both the tidal fluctuation of the beach groundwater table and movement of interface between saltwater and freshwater in both coastal confined and unconfined heterogeneous aquifers. The sharp interface philosophy is adopted to simulate dynamics of freshwater flow. Tidal waves are simulated by simple harmonic motions in time. The solution is based on an approach of separating large and small time scales motions of groundwater fluctuations. The proposed model consists of two sub-models. The first one applied Finite Element Method (FEM) to simulate the hydraulic responses of the aquifer in large time scale and it is coupled with Finite Difference Method (FDM), in the second sub-model, to simulate the corresponding ones in small time scale. The model is verified against analytical solutions presented by other previous researchers in case of homogenous aquifer. To simulate the aquifer heterogeneity, unconditional random log-hydraulic conductivity fields are generated to present different hydraulic conductivity realizations for the aquifer under consideration. The application is carried out on both the

hypothetical confined aquifer and the real Quaternary unconfined aquifer in El Arish-Rafah area, Egypt. Results show that both the groundwater fluctuation and saltwater intrusion due to tidal waves are affected by the aquifers heterogeneity and the tidal waves effects in confined aquifers are more significant than in unconfined aquifers.

**Keywords:** Saltwater intrusion, Finite Element Method, Diurnal tide, Sharp interface, Heterogeneous aquifers, Seawater fluctuations, Quaternary aquifer.

# 1. INTRODUCTION

Groundwater is considered as the main source of water supply in many coastal regions especially in arid and semi-arid zones. The irregular withdrawal of groundwater from these coastal aquifers causes a serious environmental problem called the problem of saltwater intrusion. The main causes of this problem are over-abstraction of the aquifer, which considered the main reason for the problem, short term implication (e.g. tidal effect and seismic waves), and long term implication (e.g. climate change and other periodic such as seasonal change in natural ground water) (Todd 1974). When simulating saltwater intrusion in coastal areas, the seaward boundary condition is an important factor. Most of previous studies, assumed that the coastal boundary water level is equal to the Mean Sea Level (M.S.L) neglecting tidal waves effect. Coastal groundwater is influenced by tidal cycle. Tidal dynamics are a fundamental aspect of coastal hydrology as they induce periodic fluctuations in the water table of coastal aquifers. As tidal signals propagate through an aquifer, the position of the interface between saltwater and freshwater changes, accordingly. Thus, the seaward boundary conditions must be modified to include tidal boundaries considering tidal fluctuation (Chen and Hsu 2004). Consequently, the planning and management of coastal aquifers require special treatment.

Several researchers have attempted to simulate the physics of groundwater flow process in coastal aquifers. Most of these models are based on either analytical or numerical solutions of the Boussinesq equation under several assumptions such as uniform thickness of homogenous aquifer and a single inland boundary condition at which water table oscillations are reduced to zero. Dominick et al. (1971) presented a numerical solution of Boussinesq equation, using implicit finite difference method, to simulate beach water table response to tidal forcing. The proposed model was developed for a beach with a vertical face. Fang et al. (1972) used a two dimensional finite element model to simulate the beach water table response due to tidal fluctuations, in the coastal homogenous aquifer with a vertical beach face. Philip (1973) and Smiles and Stokes (1976) pointed out the nonlinear influence of a sinusoidal tidal motion on a vertical shoreline, which will cause the water table to rise above mean sea level. Nielsen (1990) developed an analytical solution for the one dimensional Boussinesq equation for aquifers of sloping beach case. He derived a perturbation solution for small amplitude water table fluctuations based on the linearized Boussinesq equation by matching a prescribed series solution with the moving boundary condition. Two assumptions were considered: water table oscillations die out far from the coastline and the exit point of the water table on the beach face coupled with the tidal sea level is used to define the seaward boundary condition. Li et al. (1997) presented a boundary element model for studying the effect of tidal waves on groundwater table fluctuations near the beach. Their model is based on solving two dimensional fully saturated flow equations subjected to free and moving boundary conditions, including the seepage dynamics at the beach face. Ataie-Ashtiani et al. (1999) used a variable density groundwater model to analyze the effects of tidal

fluctuations on saltwater intrusion in an unconfined aquifer. They concluded that the effects of tidal fluctuations are more significant for aquifers having sloping beach face than for aquifers of vertical beach face. Li et al. (2000) presented a simplified one dimensional linearized model for Boussinesq equation. This model transforms the Boussinesq equation to an Advection Diffusion Equation (ADE) with an oscillating velocity. The perturbation method is applied to the propagation of spring neap tides in the aquifer. Wang and Tsay (2001) developed a mathematical model to evaluate tidal effect on groundwater motion and sharp interface between freshwater and saltwater in coastal aquifers. The proposed model based on an approach of separating large and small time scale motions of groundwater fluctuations. Jeng et al. (2002) derived an analytical solution for tidal fluctuations in a coupled coastal aquifer system consisting of a semi confined aquifer, a thin semi permeable layer and a phreatic aquifer. They studied the interactions, via leakage, between the confined and unconfined aquifers in response to tides. They concluded that, under certain conditions, leakage from the confined aquifer can affect considerably tidal water table fluctuations in the phreatic aquifers and vice versa. Numerical study of tidal effect on saltwater intrusion in confined and unconfined aquifers were presented by Chen and Hsu (2004). They developed a two-dimensional time independent finite difference model considering sloped beach face. Guo et al. (2010) derived an analytical solution to study groundwater fluctuations due to tidal waves. The application was carried out on a semi-infinite single aquifer comprising two different homogenous zones. Chuang et al. (2010) extended the conceptual model given by Geo et al. (2010) to a leaky aquifer system divided into a finite number of horizontal regions. Yeh et al. (2010) developed a new analytical model for simulating the water table fluctuations in anisotropic tidal unconfined aquifer. Monachesi and Guarracino (2011) presented both an exact and approximate analytical solutions for tidal waves to study head fluctuations in a coastal confined aquifer having hydraulic conductivities increasing linearly with the distance to the coastline. Aghbolaghi et al. (2012) developed a new analytical solution for Boussinesq equation to simulate the groundwater fluctuation in coastal aquifers of sloping beach face which consists of an upper unconfined aquifer, a lower confined aquifer and an aquitard in between. They concluded that, the effect of bed sloping on groundwater fluctuations and time lag is significant in case of the unconfined aquifer and not negligible if the leakage in the confined aquifer is large. Kuan et al. (2012) presented both laboratory and numerical models to study the tidal effects on the behavior of the saltwater wedge in unconfined aquifers. The laboratory results were used to test the numerical model and then it used to simulate the tidal influence on the saltwater wedge in a field scale aquifer system.

The main objective of this research is to study the tidal effects on both groundwater table fluctuations and saltwater intrusion assuming sharp interface between freshwater and saltwater. The novelty of the current research stems from developing a two-dimensional model in plan for both coastal heterogeneous confined and unconfined aquifers. The proposed model is applied on a case study of Quaternary aquifer in El Arish-Rafah area, Egypt.

# 2 NUMERICAL MODEL

Wang and Tsay (2001) presented a numerical model based on an approach of separating large and small time scale motions of groundwater fluctuations. Their model methodology is adopted in the present study with the following main modifications:

- Two-dimensional model in plan is considered in the application;
- The effect of tidal waves is studied on both groundwater fluctuations and saltwater intrusion;

- Effect of aquifer heterogeneity is taken into considerations; and
- The application is carried out on both confined and unconfined aquifers.

Figure (1) shows a definition sketch of the studied coastal aquifers. Each one is divided into two zones. Zone (1) consists of the freshwater aquifer between the impermeable layer and groundwater table with no intervening saltwater and zone (2) consists of the freshwater between groundwater table and the underlying saltwater.

The following assumptions are taken into consideration for developing the proposed model: (1) The impervious bed of the aquifer was considered horizontal, (2) The sharp interface between saltwater and freshwater is adopted, (3) the Dupuit's assumption is employed to vertically integrate the flow equation, reducing it from three dimension geometry to two dimensional geometry, (4) The Ghyben-Herzberg assumption of stagnant saltwater is utilized to interpret the interface location, and (5) The exit point of the water table on the beach face is assumed to be coupled with the tidal sea level to define the seaward boundary condition.

## 2.1 Governing Equations and Boundary Conditions

The equation of mass conservation can be written as follows (Wang and Tsay 2001):

$$\left(\frac{\partial Q_x}{\partial x}\right)+\left(\frac{\partial Q_y}{\partial y}\right)-N=-S\frac{\partial h}{\partial t} \qquad (1)$$

in which, $Q_x$ and $Q_y$ are the flow rates of the water in the two directions; $N$ is the recharge or withdrawal per unit surface area; $S$ is the storage coefficient (dimensionless) and $h$ is the piezometric head of ground water equal to $(z+p/\gamma)$; $z$ is the elevation from a specified datum; $p$ is the pressure; $\gamma$ is the specific weight; and the subscripts $x$ and $y$ represent quantities in both $X$ and $Y$ directions, respectively.

In reality, the time scale of groundwater movement is much larger than that of tidal fluctuation. Consequently, it is assumed that both the discharge $(Q)$ and piezometric head $(h)$ can be divided into two components as follows; large time scale ($Q_L$ and $h_L$) and small time scale ($Q_S$ and $h_S$), as follows:

$$Q = Q_L + Q_S \qquad (2)$$

$$h = h_L + h_S \qquad (3)$$

In the present study, the rainfall intensity/point recharge and uniform evaporation /point pumping will be treated in the equation of large time scale. Accordingly hydraulic head $h_L$ vary on a large time scale. While, groundwater fluctuations due to tidal waves will be treated in the equation of small time scale.

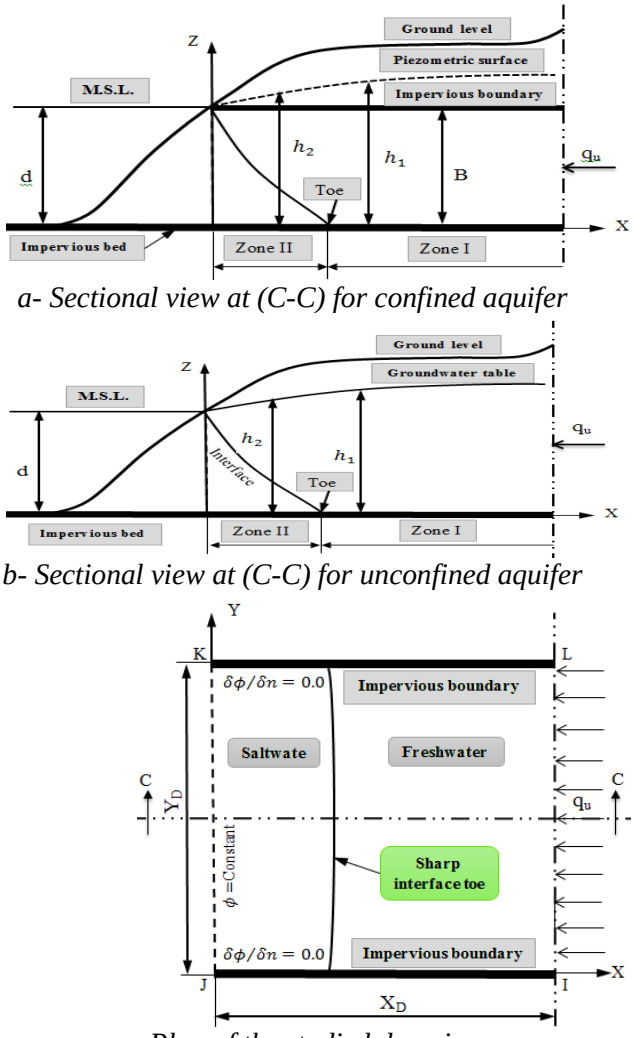


*a- Sectional view at (C-C) for confined aquifer*

*b- Sectional view at (C-C) for unconfined aquifer*

*c- Plan of the studied domain*

***Figure 1**: Definition sketch for the studied confined and unconfined aquifers*

Accordingly hydraulic head $h_S$ vary on a small time scale.
According to the previous treatment, the ground water motion can be described by the following two equations, or on other words Eq. (1) can be transformed into two equations as follows:

$$\left(\frac{\partial Q_{Lx}}{\partial x}\right)+\left(\frac{\partial Q_{Ly}}{\partial y}\right)-N=-S\frac{\partial h_{Lt}}{\partial t}$$

for large time scale (4)

$$\left(\frac{\partial Q_{Sx}}{\partial x}\right)+\left(\frac{\partial Q_{Sy}}{\partial y}\right)=-S\frac{\partial h_{St}}{\partial t}$$

for small time scale (5)

where, $h_{Lt}$ and $h_{St}$ are the hydraulic heads corresponding to large and small time scales, respectively.

<u>*For large time scale*</u>: Variation of hydraulic head ($h_{Lt}$) with respect to time, Eq. (4), is slowly varied compared with the corresponding term, in Eq. (5). Then Eq. (4) can be viewed as steady. Taigbenu et al. (1984) deduced two equations based on Eq. (4) for the two zones as follows:

*for confined aquifer:*

$$\frac{\partial}{\partial x_i}\left(K*B\frac{\partial h_{L1}}{\partial x_i}\right)-N=0$$

for zone (1) (6)

$$\frac{\partial}{\partial x_i}\left[K*\left(\frac{1}{2}\frac{\gamma_f}{\Delta\gamma}h_{L2}+B-\frac{\gamma_s d}{\nabla\gamma}\right)\right]\frac{\partial h_{L2}}{\partial x_i}-N=0$$

for zone (2) (7)

*for unconfined aquifer:*

$$\frac{\partial}{\partial x_i}\left(\frac{1}{2}K\frac{\partial h_{L1}}{\partial x_i}\right)-N=0.0$$

for zone (1) (8)

$$\frac{\partial}{\partial x_i}\left[\frac{K\gamma_s}{\Delta\gamma}*\left(\frac{{h_{L2}}^2}{2}-dh_{L2}\right)\right]\frac{\partial h_{L2}}{\partial x_i}-N=0$$

for zone (2) (9)

in which, $x_i$ coordinate axes in x and y directions; $K$ represents hydraulic conductivity; $B$ is the thickness of the confined aquifer ; $h_{L1}$ and $h_{L2}$ are the freshwater heads in zone (1) and zone (2) respectively; $\Delta\gamma=(\gamma_s-\gamma_f)$; $\gamma_f$ and $\gamma_s$ are the specific weights of the freshwater and saltwater, respectively, and $d$ is the elevation of the (M.S.L) from a specified datum.
Strack (1976) deduced only one equation to simulate the groundwater flow in both the two zones by replacing both the dependent variable $h_{L1}$ and $h_{L2}$ with the potential $\emptyset$ as follows:

$$-\frac{\partial}{\partial \mathrm{x}}\left(\mathrm{K}\frac{\partial \emptyset}{\partial \mathrm{x}}\right)-\frac{\partial}{\partial \mathrm{y}}\left(\mathrm{K}\frac{\partial \emptyset}{\partial \mathrm{y}}\right)=\mathrm{N} \qquad (10)$$

Minus sign indicates that, the flow is in decreasing head direction. Values of both $h_{L1}$ and $h_{L2}$ can then be calculated from the following equations:

*for confined aquifers:*

$$h_{L1}=\left(\emptyset-\frac{\Delta\gamma B^2}{2\gamma_f}+\frac{\gamma_s B d}{\gamma_f}\right)/B$$

for zone (1) (11)

$$h_{L2}=\sqrt{\frac{2\emptyset\Delta\gamma}{\gamma_f}+\frac{\gamma_s d}{\gamma_f}-\frac{\Delta\gamma B^2}{\gamma_f}}$$

for zone (2) (12)

*for unconfined aquifer:*

$$h_{L1}=\sqrt{2\emptyset+\frac{\gamma_s}{\gamma_f}d^2}$$

for zone (1) (13)

$$h_{L2}=\sqrt{\frac{2\emptyset\Delta\gamma}{\gamma_s}}+d$$

for zone (2) (14)

Under steadiness assumption at the interface toe, Figure (1), both $h_{L1}$ and $h_{L2}$ equal to $(\gamma_s d/\gamma_f)$. Then, $\emptyset_{toe}$ can be computed as follows, Taigbenu et al. (1984):

$$\emptyset_{toe}=\frac{\Delta\gamma B^2}{2\gamma_f} \quad \text{for confined aquifer} \qquad (15)$$

$\emptyset_{toe} = \frac{\gamma_s \Delta \gamma d^2}{2\gamma_f{}^2}$ for unconfined aquifer (16)

The following boundary conditions are considered for solving Eq. (10).
Neumann B.C:
$\partial\emptyset/\partial n = q_u/K$ (On side IL) (17)
$\partial\emptyset/\partial n = 0.0$ (On side IJ, LK) (18)
Dirichlet B.C:
$\emptyset = 0$ (On side JK) (19)
in which, $q_u$ represents uniform rate of recharge per unit width of the aquifer.

<u>*For small time scale:*</u> the following equations were derived from Eq. (5) as given by Wang and Tsay (2001).

*for confined aquifer:*

$$\frac{\partial}{\partial x}\left(B\frac{\partial h_S}{\partial x}\right) + \frac{\partial}{\partial y}\left(B\frac{\partial h_S}{\partial y}\right) = \frac{S}{K}\frac{\partial h_S}{\partial t} \quad (20)$$

*for unconfined aquifer:*

$$\frac{\partial}{\partial x}\left(h_L\frac{\partial h_S}{\partial x}\right) + \frac{\partial}{\partial y}\left(h_L\frac{\partial h_S}{\partial y}\right) = \frac{S}{K}\frac{\partial h_S}{\partial t} \quad (21)$$

The following boundary conditions are considered:
Neumann B.C:
$\partial h_S/\partial n = 0.0$ (On side IL) (22)
$\partial h_S/\partial n = 0.0$ (On side IJ, LK) (23)
Dirichlet B.C:
$h_S = \sum_{i=1}^{J} H_i \cos(\omega_i t - r_i)$
(On side JK) (24)
in which, $J$ is the number of tidal constituents; $H_i$ is the amplitude of each constituents; $\omega_i$ is the angular frequency equal to $(2\pi/T_i)$; $T_i$ is the tidal period; $t$ time and $r_i$ is the phase of tidal constituents.

The proposed model, in this research paper, is based on solving both Eq. (10), for large time scale, and Eq. (20) or Eq. (21), for small time scale, separately under the previously given boundary conditions. Then the total piezometric head ($h$) can be obtained by superposition of piezometric heads for both small and large time scales.

## 2.2 Model Formulations

The Finite Element Method (FEM) is adopted to solve Eq. (10) for large time scale and is again coupled with a fully backward Finite Difference Method (FDM), in time, to solve the governing Eq. (20) or Eq. (21) in small time scale. FEM can handle any domain with complex boundaries. Also, heterogeneity and anisotropic characteristics can easily be included. The idea of the FEM is to discretize the domain under consideration to number of elements. Rectangular elements "bounded with four nodes" were chosen in the present work. A trial function is assumed to simulate the dependent variable within different elements. This trial function is usually assumed as a polynomial with a degree specified from number of nodes per element. A weak form for the governing equation should be constructed. Galerkin form is selected, by minimizing the residuals of the selected weak solution at different nodes; the unknown dependent variables can be estimated (Burnett 1987).

Based on the FEM procedures, Eq. (10) can take the following matrix form:

$$[A] \times [\Phi] = [F] \quad (25)$$

in which: $A$ is a square matrix for the coefficients known as stiffness matrix; $\Phi$ is the unknown vector of potential and $F$ is a vector which contains the boundary fluxes.

Also based on both the FEM and FDM procedures, the matrix form of Eq. (20) or Eq. (21) is as follows

$$\left[\frac{1}{\Delta t_n}[C] + [A]\right]\{H_s\}_n = [F]_n + \frac{1}{\Delta t_n}[C]\{H_s\}_{n-1} \quad (26)$$

in which, $C$ is the capacity matrix; $H_s$ is the unknown vector of head fluctuations, $\Delta$t is the time step equal to $(t_n - t_{n-1})$,

$n=0,1,2,.....i$ and $i$ is the number of time intervals.

An original code is written using the FORTRAN language to program the proposed model. This code implements the principles of FEM in the first sub-model of large time scale and again implements both the coupled FEM and FDM procedures in the second sub-model of small time scale. The flow chart of the proposed model is presented in Figure (2).

# 3. HYPOTHETICAL CONFINED AQUIFER

The developed model is applied on the hypothetical confined aquifer similar to that shown in figure (1). The following data can be assumed: the dimensions of the studied domain are 2000 m in both *x*-direction and *y*-direction, height of the (M.S.L) from a specified datum ($d$) equal to 15.0 m, thickness of the confined aquifer ($B$) equal to 15.0 m, density of saltwater ($\gamma_s$) is 1025 $Kg/m^3$, density of freshwater ($\gamma_f$) is 1000 $Kg/m^3$, storativity ($S$) is 0.002 (Dimensionless), and the uniform recharge through the aquifer ($q_u$) equals 0.6 $m^3/d/m$.
The tide data are assumed as follows: Amplitude of sea level ($A$) equal to 1.0 m, angular frequency ($\omega$) equals ($2\pi/T$) Rad $h^{-1}$, phase of tidal constituents ($r_i$) equal to ($\pi/2$) and period ($T$) equal to 24 hours. In the following three sub-sections the studied confined aquifer is considered homogenous of hydraulic conductivity ($K$) equal to 100 m/day.

### 3.1. Meshing and Time Independent Test

Several trials are carried out to select both the suitable mesh size and time step ($\Delta t$). In each trial, water table fluctuations at different locations are calculated. It is found that, the results are independent on both mesh size and time step when the mesh is discretized to 1600 elements and $\Delta t$ = 0.1 hr. To demonstrate that these chosen valued are actually the suitable, the solution is repeated with smaller grid sizes and time step (mesh size is taken equal to 6400 elements and $\Delta t$ = 0.05 hr). Figure (3) shows water table fluctuations at different locations, in the studied domain, considering the two mesh sizes and time steps. As seen in this figure, the difference between water table fluctuations in all the considered locations is insignificant.

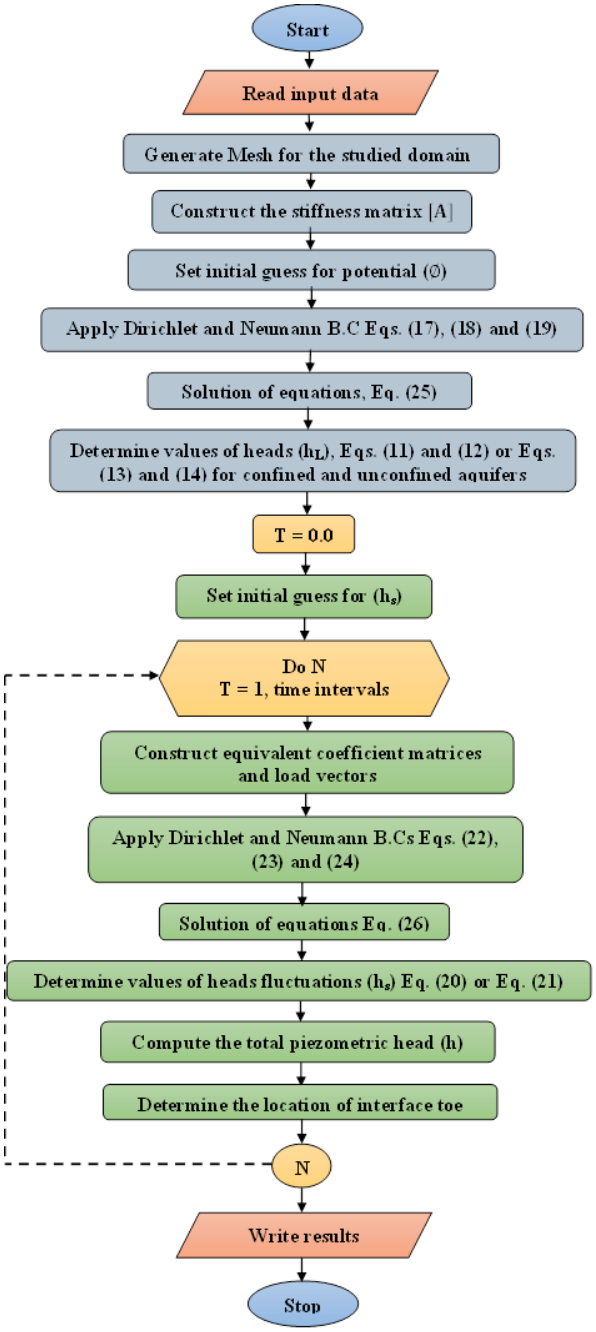


***Figure 2:*** *Flow chart for the proposed model*

### 3.2. Periodicity of the Solution

Initial values for water table should be assumed at zero time to possibility solve Eq. (26). At zero time, it is assumed that there is no fluctuations in water table and then $h_s$= 0.0 at $t$ = 0.0. The effect of these initial values on the solution are diminished after a certain time (called memory time, $t_c$) elapses and the solution becomes periodic. Figure (4.a) shows head fluctuations at three different locations through the studied domain for the first four tidal periods. To insure that the solution becomes periodic, the difference of the predicted head fluctuations between each two subsequent periods are calculated until this difference is nearly equal to zero, Figure (4.b). As seen in this figure, it is sufficient to ensure the solution's periodicity if *t* three times larger than the tidal period (*T*).

### 3.3. Model Verification

The proposed model presented in this paper is built on solving both Eq. (10) and Eq. (20) separately and their results are added (Wang and Tsay 2001). Consequently, the verification of the numerical solution for each equation is carried out separately. The numerical solution of Eq. (10) is verified against the analytical solution using the potential flow theory (Strack 1976). While, the analytical solution given by Nielsen (1990) is used to verify the numerical solution of Eq. (20). The relative absolute average error between the analytical and numerical solutions is determined using the following equation in both cases separately:

$$error = \frac{\sum_{i=1}^{m} \frac{|h_{Ai} - h_{Ni}|}{h_{Ai}}}{n} \qquad (27)$$

in which, $h_{Ai}$ is the head node *i* calculated from analytical solution; $h_{Ni}$ is the head at node *i* calculated from numerical solution and *n* is the number of nodes through the studied domain.

*For large time scale:* the potential $\emptyset$ due to uniform recharge ($q_u$) through the boundary *IL*, Figure (1-c), can be represented as:

$$\emptyset = \emptyset_0 + \frac{q_u}{K} X \qquad (28)$$

where, $\emptyset_0$ is the initial value of $\emptyset$ at boundary *JK*, equal to zero because there is no seepage face at the sea coast. The values of the potential $\emptyset$ resulted from both analytical and numerical methods are calculated and compared. The relative absolute average error between numerical and analytical results is found to be equals: $1.75\times10^{-5}$.

*For small time scale:* the analytical solution for the Boussinesq equation as given by Nielsen (1990) for vertical beach is as follows:

$$h_S(x,t) = Ae^{(-kx)}\cos(\omega t - r - kx) \qquad (29)$$

where:

$$k = \sqrt{S\omega/2KB}$$

in which, $h_S$ is the head fluctuations and $k$ is the amplitude damping coefficient of one-dimension tidal head fluctuations.

Figure (5) shows the tidal head fluctuations resulted from both the analytical and numerical solutions at different locations. Also, the corresponding errors are listed. As seen in all figures, both the analytical and numerical solution agrees very well with each other.

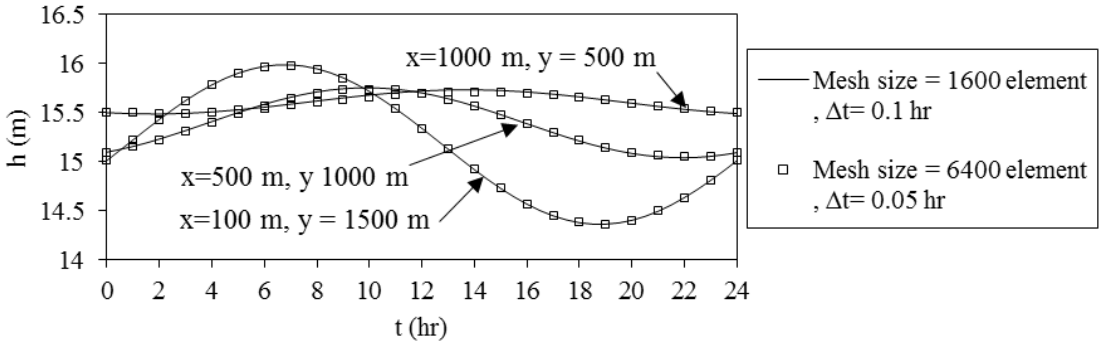


***Figure 3:*** *Comparison of water table fluctuations using different mesh sizes and time steps at different locations*

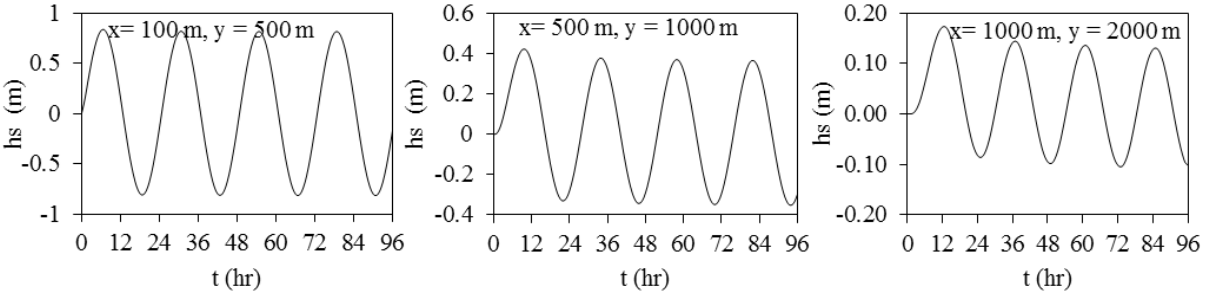


*(a) Head fluctuation for the first four tidal periods at several locations*

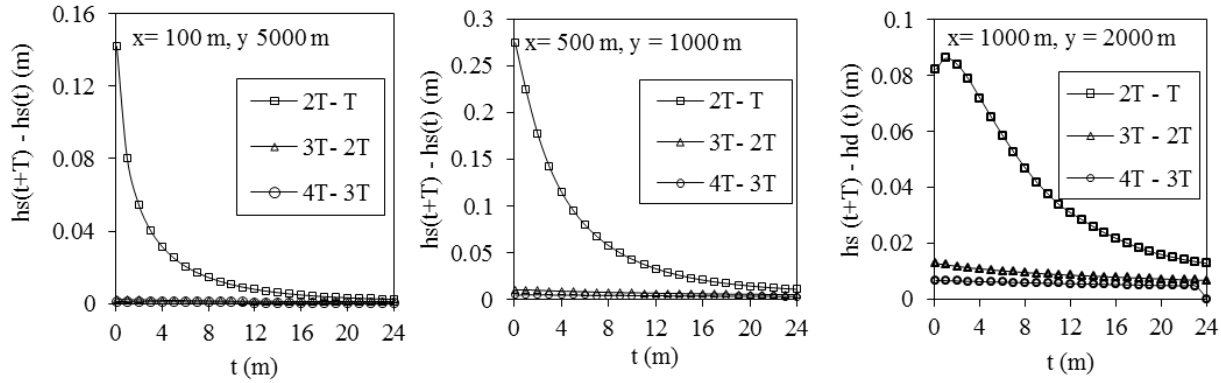


*(b) Differences of the predicted head fluctuations between each two subsequent periods several locations*

***Figure 4:*** *Periodicity of solution*

### 3.4. Heterogeneity of the Aquifer

Heterogeneity of the aquifer means that, the hydraulic conductivity at any point within the aquifer is different from the other points. Within the FEM any studied aquifer can be considered heterogeneous by adopting different magnitudes of hydraulic conductivity for every element. Hydraulic conductivity within any element of the studied aquifer is created from a normal random distribution. The logarithms of hydraulic conductivity can be represented by the first two moments (the mean $\mu$ and the standard division $\sigma$) as follows (Abdel-Gawad 1999):

$$\ln K_1 = \mu + u_1\sigma \,, \ln K_2 = \mu + u_2\sigma \qquad (30)$$

where:

$$u_1 = (-2\ln\varepsilon_1)^{1/2}\cos(2\pi\varepsilon_2),$$
$$u_2 = (-2\ln\varepsilon_1)^{1/2}\sin(2\pi\varepsilon_2)$$

in which, $u_1$ and $u_2$ are normally distributed random numbers with mean equal to 0 and standard division equal to 1; and $\varepsilon_1$ and $\varepsilon_2$ are independent uniform random numbers distributed in range from 0 to 1.

### 3.5 Discussion of Tidal Propagation on Heterogeneous Confined Aquifer

Each diurnal tidal cycle consists of four stages, Figure (6). In the first stage, between t = nT and t = (n+1/4)T, the sea level rises from mean sea level to its highest level. In the second stage, between t = (n+1/4)T and t = (n+1/2)T, the sea level falls from its highest level to its original mean. In the third stage, between t = (n+1/2)T and t = (n+3/4)T, the sea level falls to its lowest level. In the last stage, between t = (n+3/4)T and t = (n+1)T, the sea level rises again, reaching to its mean sea level at t= (n+1) T, where, n = 0, 1, 2,…… number of tidal cycles.

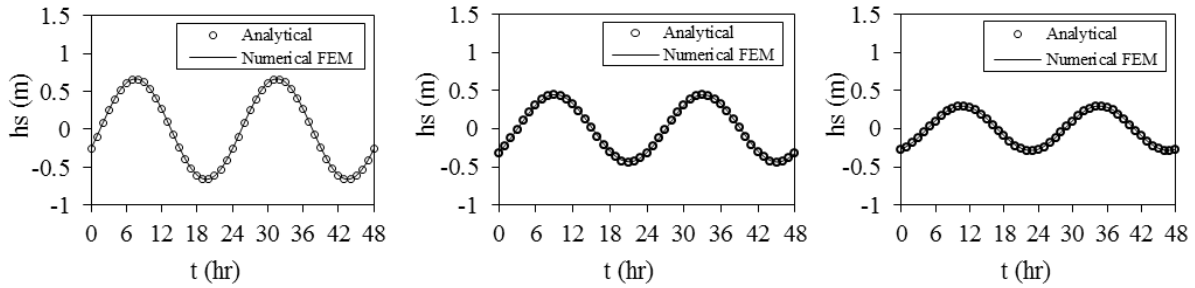


a- x=200m, y = 500 m and error = $1.48\times10^{-3}$

b- x=400m, y = 1500 m and error = $3.0\times10^{-4}$

c- x=600m, y = 300 m and error = $3.95\times10^{-3}$

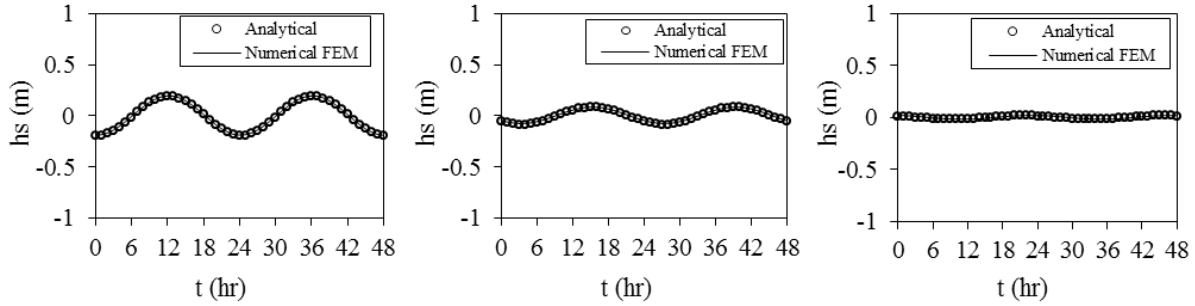


d- x=800m, y = 1000 m and error = $2.72\times10^{-3}$

e- x=1200m, y = 700 m and error = $6.9\times10^{-2}$

f- x=2000m, y = 1800 m and error = $3.2\times10^{-2}$

***Figure 5:*** *Tidal head fluctuations resulted from both analytical and numerical solutions*

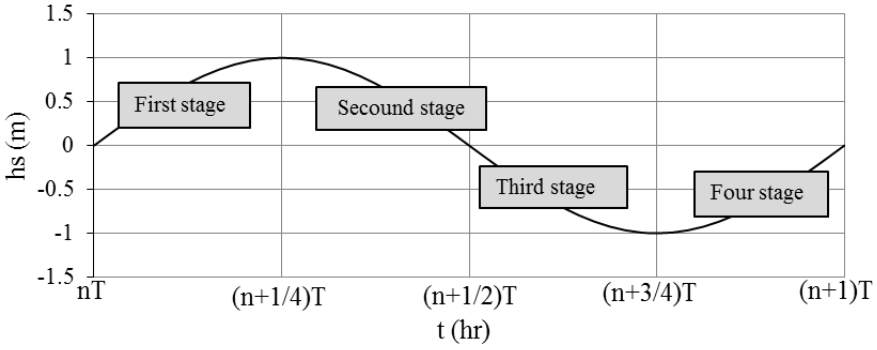


***Figure 6:*** *Fluctuation of sea level elevation due to diurnal tide*

In this research six realizations were assumed. In each realization the mean $\mu$ is assumed constant equal to 4.0 while the values of standard deviation ($\sigma$) are taken equal to 0.0, 0.5, 1.0, 1.5, 2.0 and 3.0 respectively. Figures (7a-f) represent the generated hydraulic conductivities corresponding to each case of heterogeneity (i.e realization) using Eq. (30). The first realization shown in figure (7-a) means the aquifer is homogenous. The gradual different in color shown in each realization refers to difference in hydraulic conductivity through each element. From this figure, it is noted that with increasing the value of standard deviation ($\sigma$), the range of hydraulic conductivity through domain increases.

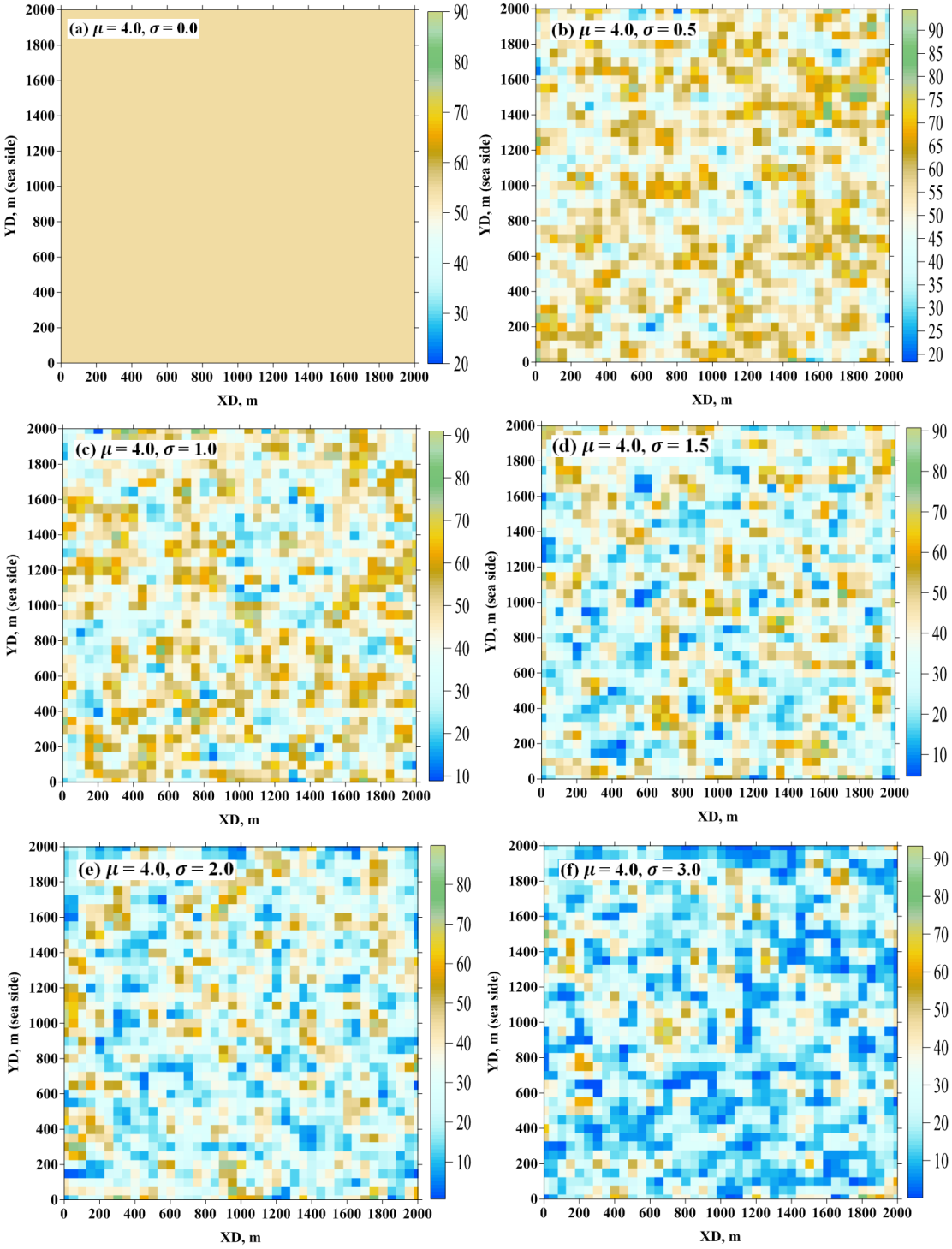


***Figure 7:*** *Hydraulic conductivity realizations for the studied heterogeneous aquifer*

As a result of sinusoidal tidal waves, the piezometric water table fluctuation are also sinusoidal wave, Figure (5), then a hydraulic term of fluctuation amplitude (A) can be estimated as follows (Li et al. 1999):

$$A = (h_{max} - h_{min})/2 \qquad (31)$$

where, A: the fluctuation amplitude; and $h_{max}$ and $h_{min}$ are the maximum and minimum height of the piezometric head due to tide at each point in the studied domain.

Figure (8) shows the fluctuation amplitude (A) corresponding to each distance inland, at cross-sectional y = 1000 m, for each case of heterogeneity. It is noticed that the fluctuation amplitude (A) reduced with increasing the distance inland for all cases of heterogeneity. This logical behavior is due to the piezometric water table is highly affected by tidal fluctuations near the coastal face and gradually decreased towards inland. Also, for increasing the value of standard deviation the value of fluctuation amplitude reduced. For example at x = 400 m values of $A$ = 0.44, 0.39, 0.30, 0.23, 0.08 and *0.008* corresponding to values of $\sigma$ equal to 0.0, 0.5, 1.0, 1.5, 2.0, and 3.0, respectively. This is due to the decrease in the estimated hydraulic conductivities in most of elements as a result of increasing the values of standard deviation, Figure (7), and in general the flow movement through porous media decreases. Therefore, the effect of tidal wave is almost vanished when $x$ equal to greater than 2000 m, 1600 m, 1200 m, 810 m, 600 m and 300 m corresponding to values of $\sigma$ equal 0.0, 0.5, 1.0, 1.5, 2.0, and 3.0, respectively.

Figures (9a-f) demonstrate contour lines of the fluctuation amplitude ($A$) for the studied domain corresponding to each case of heterogeneity. For $\sigma$ = 0.0 (i.e. homogenous aquifer), the contour lines are straight parallel to the coastline, indicating that uniform vanishing of fluctuation amplitude. This, of course, due to constant value of hydraulic conductivity, in the studied domain, and consequently the flow movement through porous media is constant (i.e. the domain is symmetric). As the values of the standard deviation increase, the contour lines take a curved shape. This happens as the flow is enforced to move with elements of high hydraulic conductivities than elements of small hydraulic conductivities. Also, as explained in the previous figure, for increasing the values of standard deviation the water table fluctuations are vanished in a smaller distances from the coast line.

Figures (10a-e) plot the movement of interface toe with respect to time, due to tidal fluctuations, for each case of heterogeneity at several cross sections. As shown in all figures, the movement of interface toe is harmonically varies with the tidal waves movement. For example, at cross section y = 500 m, Figure (10-b), when the sea level at mean sea level, the interface toe is at specified distances from the coast line for each case of heterogeneity.

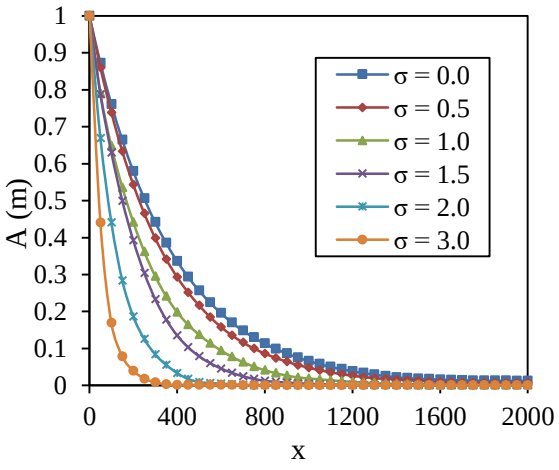


***Figure 8:*** *The fluctuation amplitude (A) corresponding to each distance inland for each case of heterogeneity (at cross-sectional y = 1000m)*

When the sea level reached to its maximum level at 0.25T, Figure (6), the interface toe is still moves towards inland for all cases of heterogeneity. When the sea level again reached to the original position at 0.5T, Figure (6), the interface toe reached to maximum intrusion length and begins to

retard towards the coast line. When the tidal level reached to its minimum level at 0.75T, Figure (6), the interface toe is still gradually retarded towards the cost line for all cases of heterogeneity. When the sea level again reached to the original position at 1.0T, Figure (6), the interface toe reached to minimum intrusion length and again begins to move towards inland. It is found that, for all cases of heterogeneity and at all cross sections, the maximum intrusion length, due to increasing tidal wave, is carried out at 0.38T with time lag equal to 0.13T while the minimum intrusion length, due to decreasing tidal wave, is performed at 0.875 T with time lag equal to 0.125 T. Figure (11a-f) demonstrated the area of interface toe movement due to tidal waves, calculated from maximum and minimum intrusion lengths, for each case of heterogeneity. It can be seen that, when the value of standard division equal to 0.0 this area is uniform parallel to the coastline. While with increasing the standard deviation, the interface toe becomes tortuous and the area of the interface toe movement decreases. This is due to increasing the element of small hydraulic conductivities, in the studied domain (Figure 7), and consequently the flow movement through element of small hydraulic conductivity is relatively smaller than in element of high hydraulic conductivity.

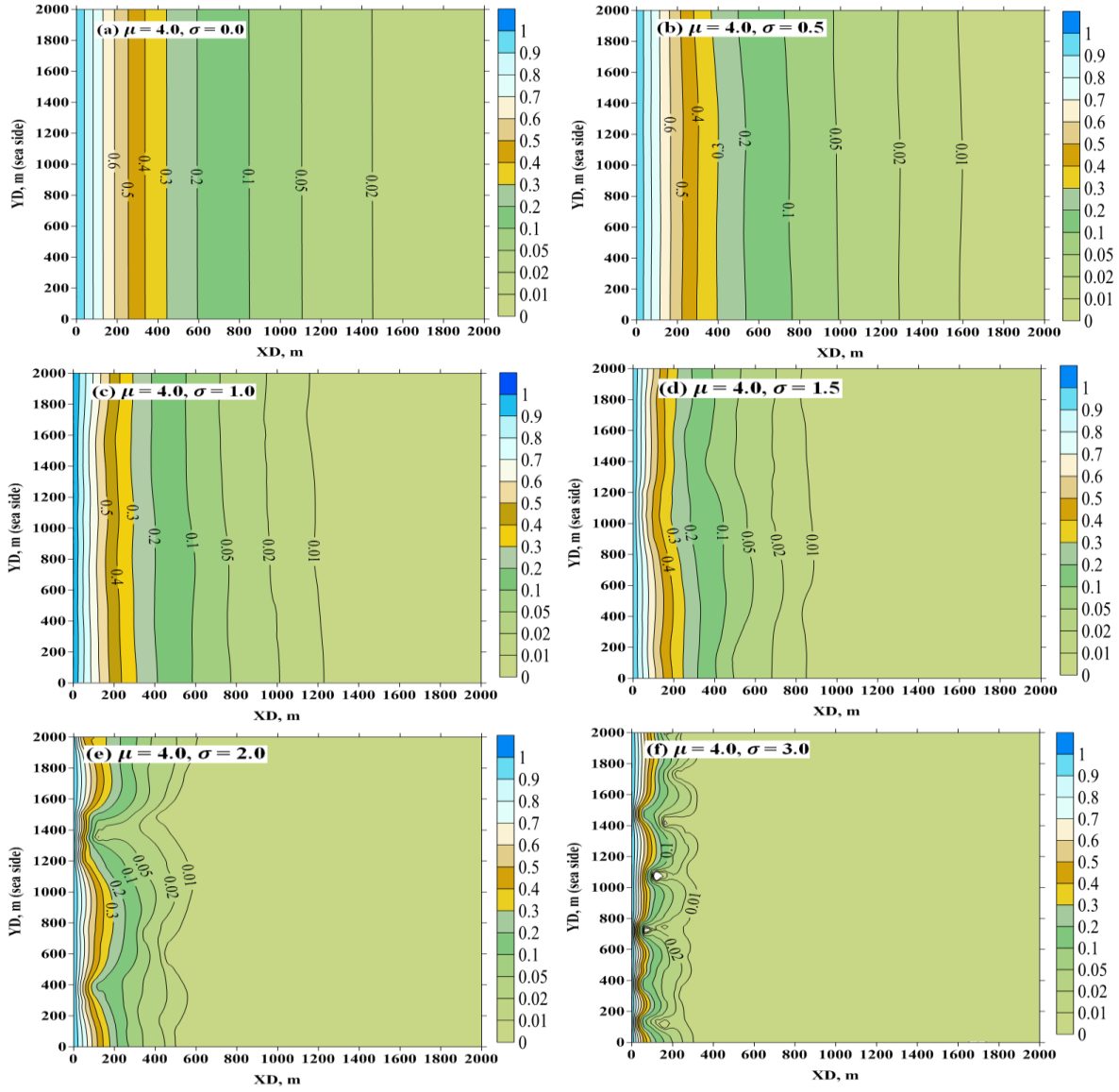


***Figure 9:*** *Contour lines of the fluctuation amplitude (A) corresponding to each case of heterogeneity*

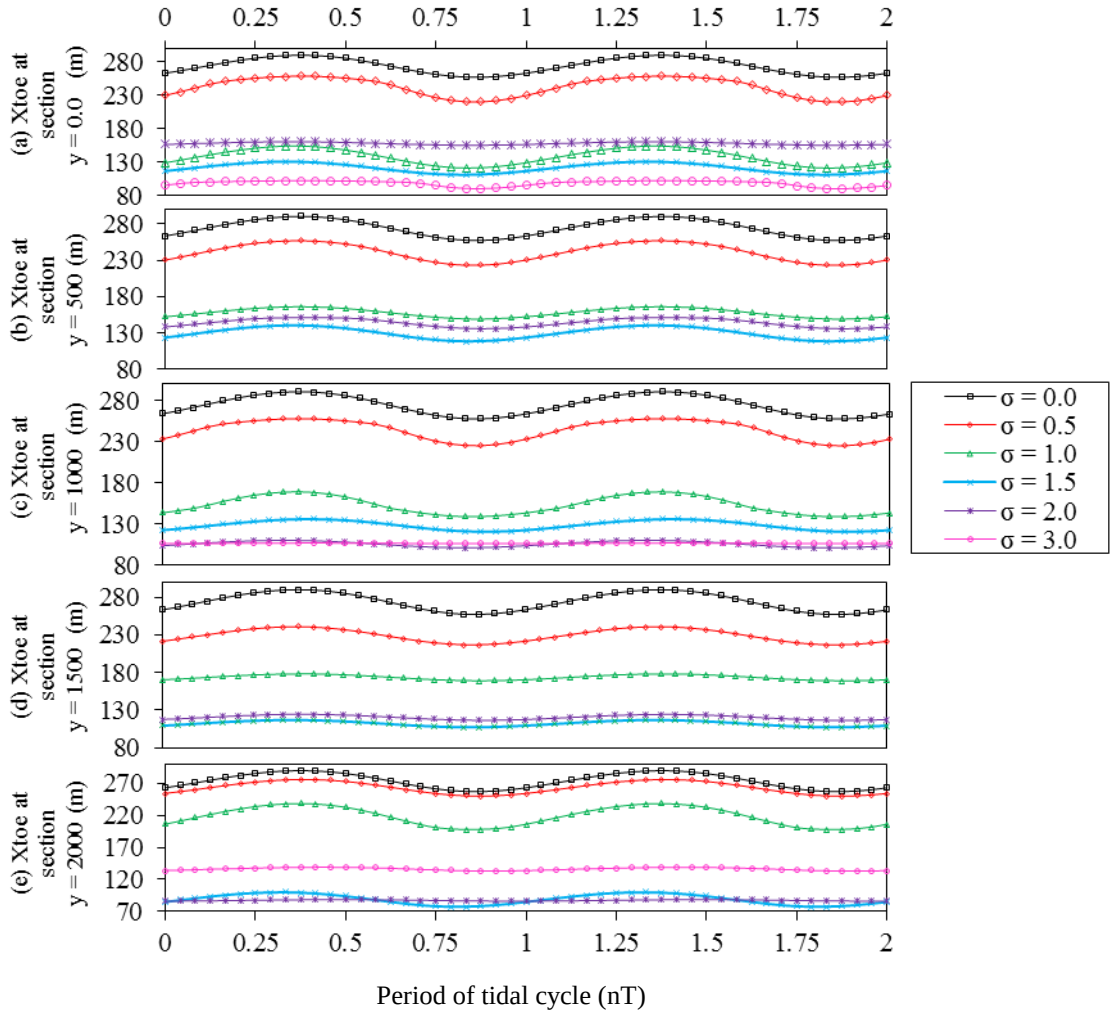


***Figure 10:*** *Variation of interface toe distance at different cross sections for every case of heterogeneity*

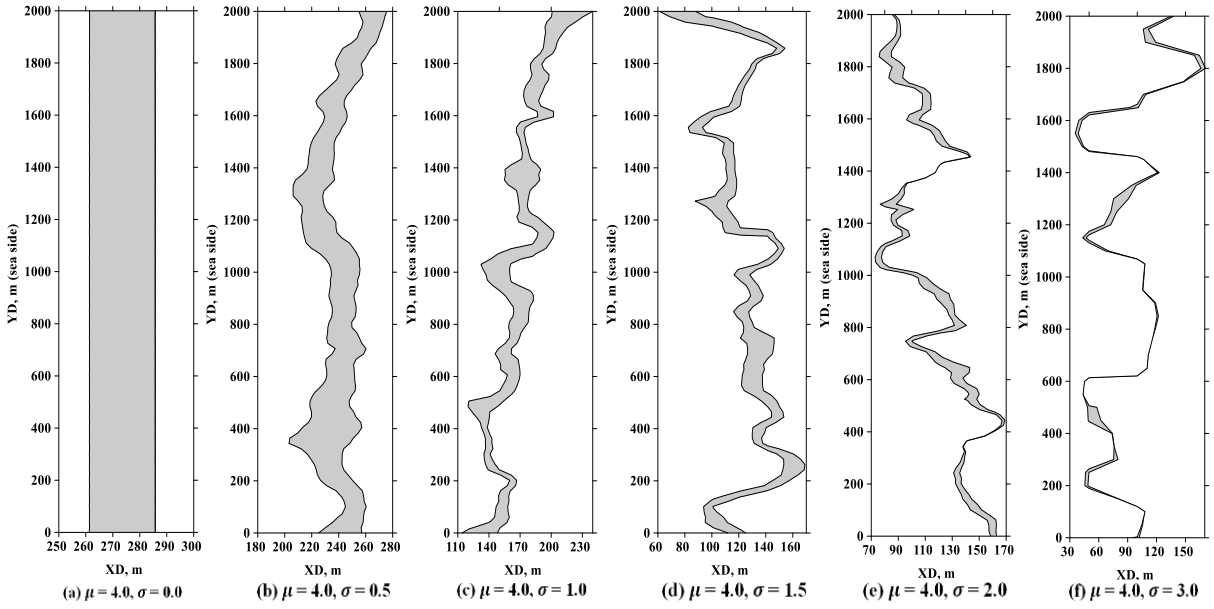


***Figure 11:*** *A fluctuations area of the interface toe between the maximum and minimum distance of intrusion for every case of heterogeneity*

# 4 CASE STUDY: QUATERNARY AQUIFER IN EL ARISH-RAFAH AREA, EGYPT

Egypt is located in the north-eastern part of the continent of Africa. Egypt's natural boundaries consist of more than 2900 kilometers of coastline along the Mediterranean Sea, the Gulf of Suez, the Gulf of Aqaba, and the Red Sea. Sinai Peninsula is a part of Egypt, which is also considered as a part of Asia continent. Sinai is approximately 380 km long and 210 km wide, and the surface area is about 61,000 km$^2$, Figure (12). The groundwater in Sinai is considered as a main source for drinking, agricultural, industrial, and other purposes.

The Quaternary aquifer in north Sinai consists of three areas: the area from Rafah to east of El Arish, the Delta El Arish valley and the area from Bir El-Abd to west Rommana, Figure (12). The three areas have different hydrogeological conditions and depositional environments.

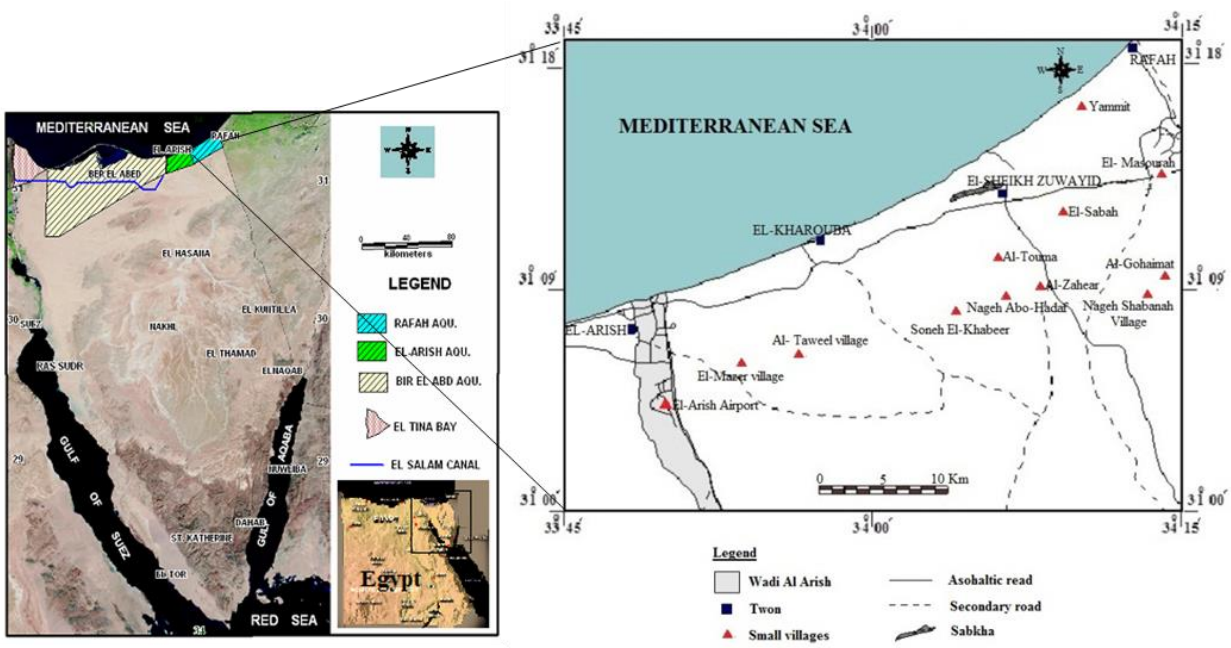


***Figure 12:*** *Map of Sinai Peninsula and location map of El Arish-Rafah area*

The coastal aquifer at El Arish-Rafah area, Figure (12), is considered to apply the proposed model. The study area encompasses about 370 Km$^2$. Lithology of El Arish-Rafah coastal aquifer is grouped into three main units, namely, sand/gravel, clay and Kurkar (i.e. calcareous sandstone). Figure (13) shows a schematic sectional view for the conceptual model of Quaternary aquifer in El Arish-Rafah area. Based on the site characterization study, it is concluded that the upper part of the aquifer is sand/gravel (sand dunes, old beach deposits, and alluvial), and the lower part consists of Pleistocene Kurkar formations. In many boreholes data the clay layer between the two formations is absent or exist in lenses in which it works as a semi-confining layer for the Kurkar formations (Abdallah 2006). In this study the coastal aquifer at El Arish-Rafah is considered as a sallow and phreatic. Vertical homogeneity is assumed so, the three layers have been merged to constitute a single equivalent layer with an equivalent thickness and hydraulic conductivity. All hydraulic parameters of the studied aquifer are obtained from the central laboratory of the Desert Research Center, Egypt, and any other missing data are reasonably assumed.

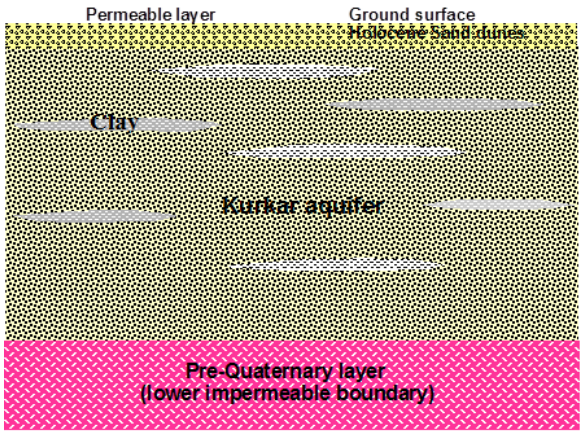


***Figure 13:*** *Schematic section showing the conceptual model of Quaternary aquifer in El Arish-Rafah area*

The studied domain dimensions are 43200 m length along the shore line and 8150 m perpendicular to it; height of the (M.S.L) from a specified datum ($d$) is equal to 40.0 m; the specific weights of saltwater ($\gamma_s$) is 1025 $Kg/m^3$; the specific weights of freshwater ($\gamma_f$) equals 1000 $Kg/m^3$; and storativity ($S$) is assumed equal to 0.01 (Dimensionless). The data corresponding to tidal waves are assumed as the same in the previous hypothetical confined aquifer.

### 4.1 Computational Grid and Boundary Conditions

Mesh generation is the main step to start the simulation procedure which the studied domain is divided into a suitable grid pattern. The model has been constructed with a rectangular grid system of 100 ×100 elements. It covers an area of 370 $km^2$. The computational grid is divided into 276 rows and 400 columns, Figure (14). As shown in Figure (14), the Mediterranean Sea borders the model area in the north. So, this boundary is defined as a constant head boundary during the study at large time scale ($\phi$=0.0). The south boundary represents the inlet of flow ($\partial\phi/\partial n=q_u/k$) where $q_u$ is the uniform rate of recharge per unit width. The eastern and western boundaries are considered as no flow boundaries ($\partial\phi/\partial n$=0.0). The seepage faces of the freshwater above (M.S.L) are ignored within the present study.

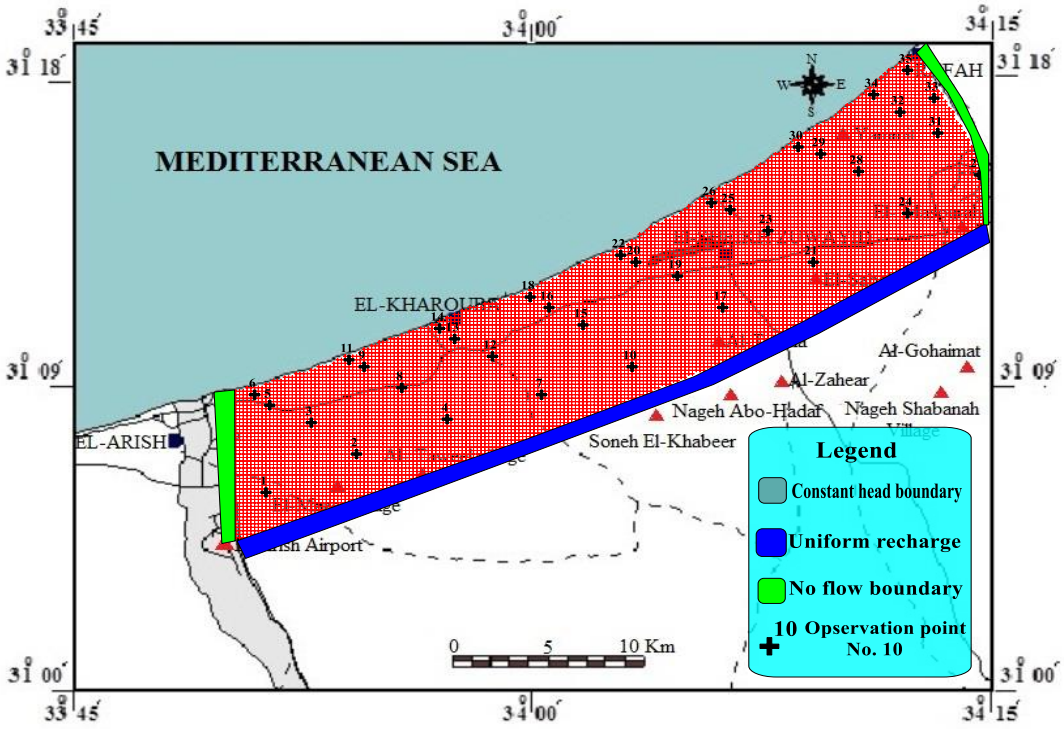


***Figure 14:*** *The grid of the studied domain for Quaternary aquifer and the used boundary conditions*

### 4.2 Model Calibration

In this section, the model is calibrated using both the available point measurements of the flow parameters and hydrological measurements collected by the central laboratory of the Desert Research Center, Egypt. In the present study, the values of hydraulic conductivity and recharge are assumed unknown flow parameters. So the model is firstly calibrated assuming steady state conditions. The collected groundwater table levels in the year of 2006 are adopted in the calibration. Recharge Zones are selected based on the analysis colors of a satellite image, Figure (15). Such color composition shows vegetated areas where expected returned irrigated water can recharge the aquifer. Calibrated recharge values should reflect recharge due to rainfall, returned water from different water uses and possible unknown recharge from other underlying formations not accounted here. As shown in Figure (15), the recharge has a maximum value of 3 $\times 10^{-3}$ m/d in the north east of the study area while, it equals to 1.2 $\times 10^{-7}$m/d in the southern boundary (Abdallah 2006). To calculate the hydraulic conductivity the values of the mean $\mu$ and the standard division ($\sigma$) in Eq. 30 are determined using the trial and error procedures until a minimum total residual error between measured and calibrated heads was achieved. The calibrated hydraulic conductivity in the studied domain is shown in Figure (16). As shown in the figure, the hydraulic conductivity ranged from 0.01 to 3 m/d. Also, it can be shown that, the zones of high hydraulic conductivity values exist in south east, north east and the middle distance between Rafah and Sheikh Zuwyied cities. The contours of calculated heads are shown in Figure (17-a). A good match between the observed heads and calculated heads is achieved as seen in Figure (17-b). The relative absolute average error (Eq.27) between the observed heads and calculated heads is found to be equals, 0.1.

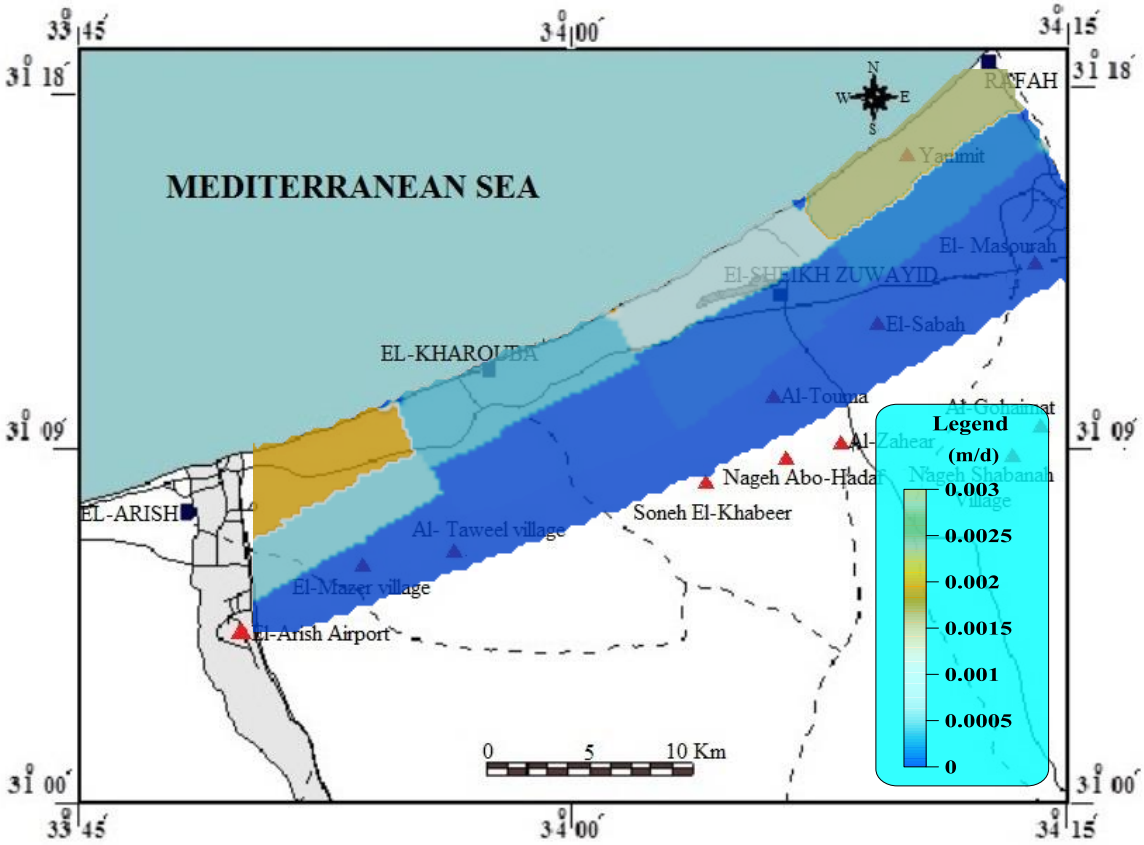


***Figure 15:*** *Calibrated recharge Zones*

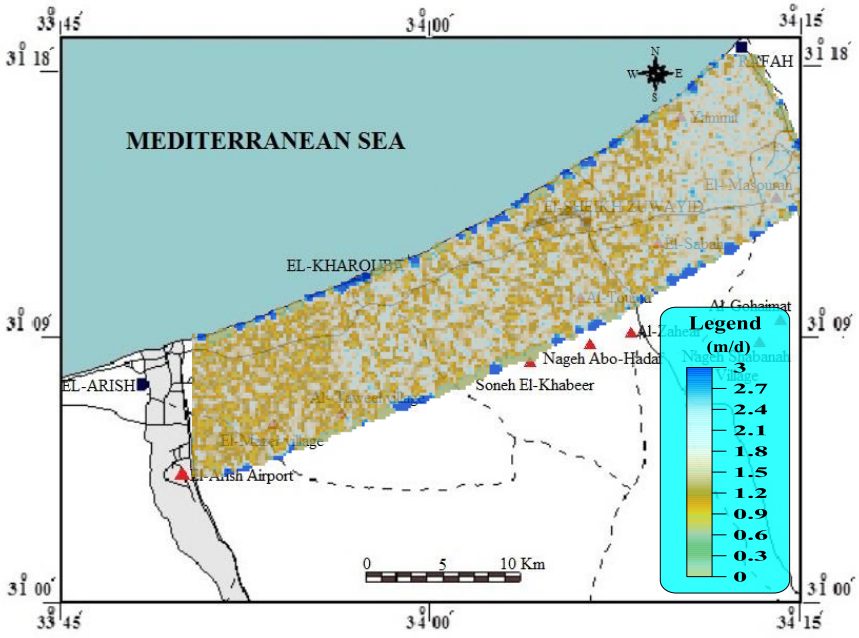


***Figure 16:*** *Calibrated hydraulic conductivity*

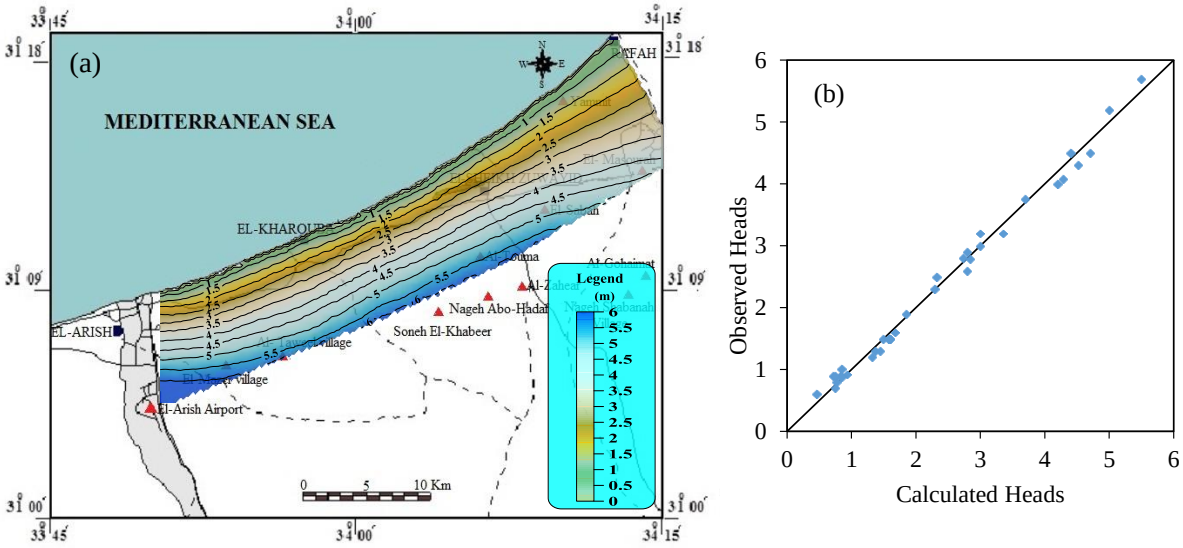


***Figure 17:*** *Contour lines of the calculated heads, and a comparison of calculated and observed heads*

### 4.3 Discussion of Tidal Propagation on Quaternary Aquifer in El Arish-Rafah Area

Figure (18) demonstrates the contour lines of the fluctuation amplitude (*A*), Eq. (31). The studied domain is divided into four regions. In region (1), near the Rafah area, the contour lines are straight parallel to the coastline, indicating that uniform vanishing of the fluctuation amplitude. This uniformity due to the difference between values of hydraulic conductivities in this region is small and it can be considered as a homogenous region, Figure (16). Consequently the flow movement in this region is uniform. In the other regions, from El-Sheikh Zuwyied to the east of El Arish areas, the contour lines take a curved shape. This may be due to the curvature of the shore line or due to the small estimated hydraulic conductivities values in most of

elements in these regions, Figure (16). Therefore, the flow is enforced to move with elements of high hydraulic conductivities than elements of small hydraulic conductivities. Also, for region (1) the water table fluctuations are vanished in a larger distances from the coast line. Because of this region is considered homogeneous compared with other regions. In general, it is concluded that the tidal wave will relatively more spread in the Rafah area than other areas.

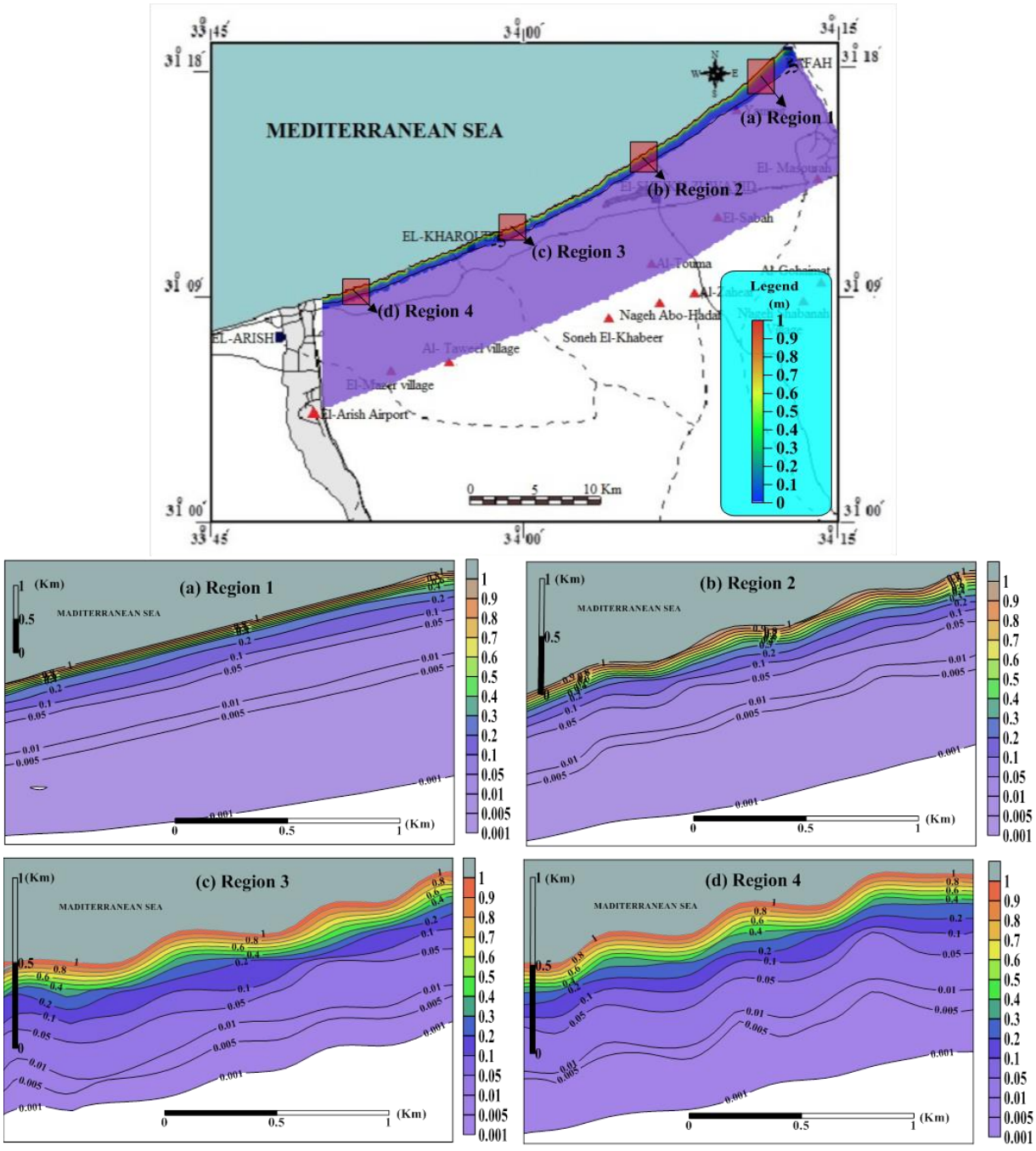


***Figure 18:*** *Contour lines of the fluctuation amplitude (A) at different four regions*

Figure (19) shows the intruded area (i.e. the contaminant area with saltwater). Four cross sectional are chosen to demonstrate the movement of interface toe with respect to time, due to tidal fluctuation. As shown in the cross sections, the movement of interface

toe are harmonically varies with the tidal wave movement as explained before in section 3. The maximum intrusion length, due to maximum tidal wave, is carried out at time equal to *0.67T hr* with time lag equal to *0.42T hr* while the minimum intrusion length, due to minimum tidal wave, is performed at time equal to *1.2T hr* with time lag equal to *0.45T hr*. Also, it can be seen that the range of groundwater fluctuations is smaller than the corresponding one in case of confined aquifer. Consequently, the effect of tidal waves on the increasing of saltwater is negligible. These conclusions were assured by other previous researchers.

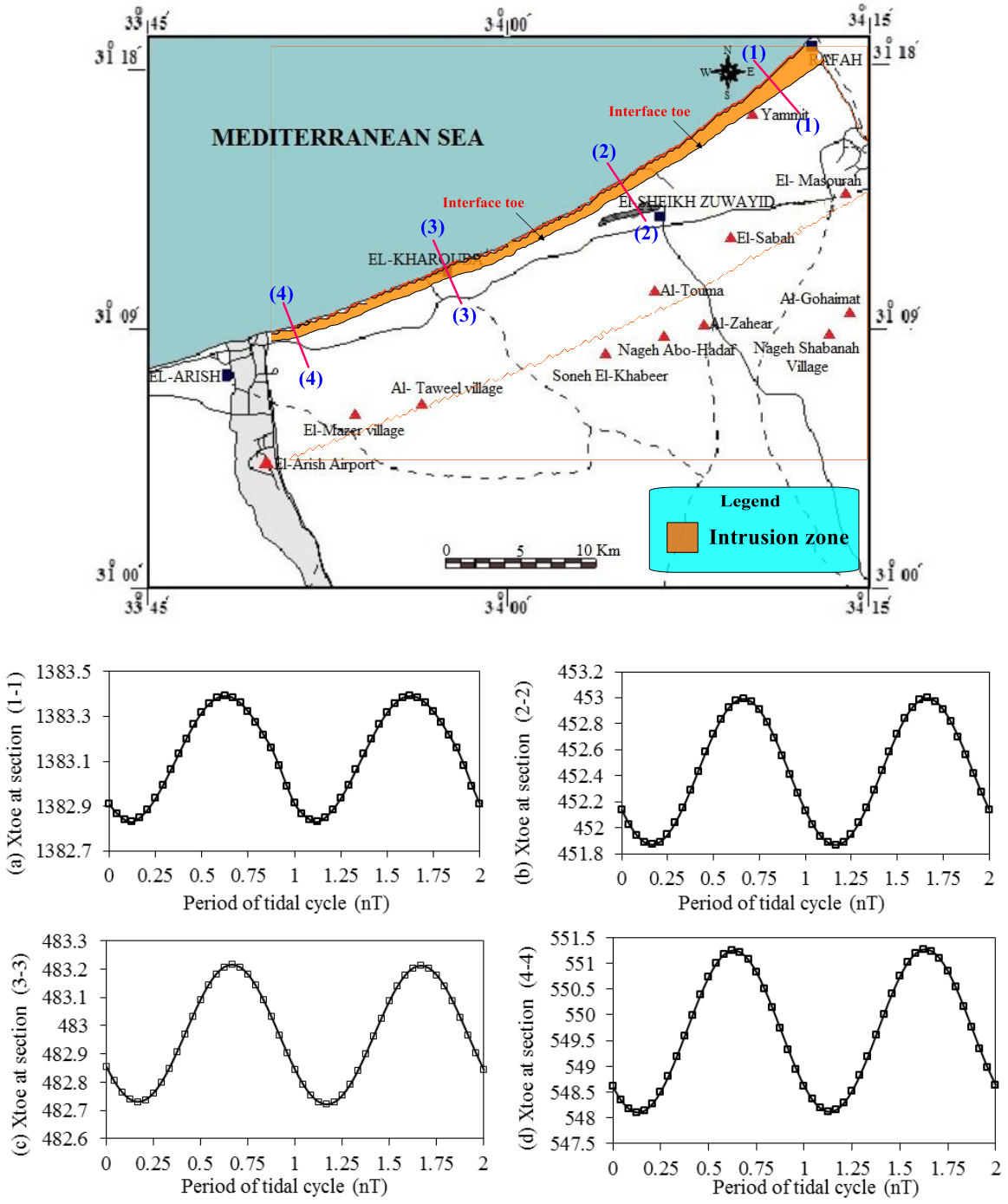


***Figure 19:*** *Variation of interface toe distance at different cross sections for every case of heterogeneity*

# 5. CONCLUSIONS

In this research, a two dimensional numerical model was modified to study the effect of tidal waves on both the groundwater fluctuation and saltwater intrusion in heterogeneous confined and unconfined aquifers. The assumption of sharp interface between saltwater and freshwater is adopted. The model is based on an approach of separating large and small time scale motions of groundwater fluctuations. Strack's formulation is applied to transform the nonlinear flow equation to linear form without any relaxation. For confined heterogeneous aquifer it is found that, with increasing the standard deviation the range of estimated hydraulic conductivities, through the studied domain, is increased and the effect of tidal wave on the ground water fluctuations is almost vanished in a smaller distances from the coast line. Also, the movement of interface toe is harmonically varies with the tidal waves movement and there is a time lag between both maximum tidal wave and maximum intrusion length; and minimum tidal wave and minimum intrusion length. Also, with increasing the standard deviation the effect of tidal waves on saltwater intrusion decreases. The developed model is calibrated and applied on the quaternary unconfined aquifer in El Arish-Rafah area, Egypt. The water table fluctuations, due to tidal waves, at Rafah area are vanished in a larger distances from the coast line than at El-Sheikh Zuwyied area. In general, the effect of tidal waves on both groundwater fluctuations and saltwater intrusion in confined aquifer is more significant than in unconfined aquifers.

# ACKNOLUGEMENT

This paper is a part of M.Sc. thesis of third author under supervision of the other authors.

The authors would like to express their deepest thanks to ***prof. Dr. Mohamed Gad***, Desert Research Centre, for his help for obtaining the real data of Quaternary aquifer.

# REFERENCES

Abdallah, G., (2006). "Management of Groundwater Aquifers along the Mediterranean Sea in Sinai Peninsula", The 2nd International Conf. on Water Resources & Arid Environment.

Abdel Gawad, H. (1999), "Deterministic and Stochastic Approaches to Inverse Problem of Groundwater Flow and Their Effect on Dispersion of Pollution", Ph. D. Thesis Slovak University of Technology, Bratislava, Slovakia, P. 135.

Aghbolaghi, M. A., Chuang, M. and Yeh, H. (2012), "Groundwater Response to Tidal Fluctuation in A sloping Leaky Aquifer System", Applied Mathematical Modeling, doi:10.1016/j.apm.2011.12.009.

Ataie-Ashtiani, B., Volker, R.E., Lockington, S. A. (1999), "Tidal Effects on Sea-Water Intrusion in Unconfined Aquifers", Journal of Hydrology 216(1-2), pp.17-31.

Burnett, D. s., (1987), "Finite Element Analysis from Concepts to Application",AT&T Bell Laboratories, P.844.

Chen, B. F. and Hsu, S. M. (2004), "Numerical Study of Tidal Effects on Seawater Intrusion in Confined and Unconfined Aquifers by Time-independent Finite Difference Method", ASCE Journal of Waterway, Port, Coastal, and Ocean Engineering, 130(4), pp.191–206.

Chuang, M. H., Huang, C. S., Li, G. H. and Yeh, H. D., (2010). "Groundwater Fluctuations in Heterogeneous Coastal Leaky Aquifer Systems", Hydrol. Earth Syst. Sci., 14, pp. 1819-1826.

Dominick, T. F., Wilkins, B. and Roberts, H. (1971), "Mathematical Model for Beach Groundwater Fluctuations", Water Resources Research 7, pp.1626-1635.

Fang, C.S., Wang, S.N. and Harrison, W. (1972), "Groundwater Flow in a Sandy Tidal Beach: Two Dimensional Finite Element

analysis", Water Resources Research 8, pp. 121-128.

Guo, H. P., Jiao, J. J. and Li, H. L., (2010). "Groundwater Response to Tidal Fluctuation in a Two-zone Aquifer" Journal Hydrology, 381, pp. 381-371.

Jeng, D.S., Li, L and Barry, D.A., (2002), "Analytical Solution for Tidal Propagation in A coupled Semi-Confined/Phreatic Coastal Aquifer", Adv. Water Resource. 25(5), pp. 577–584.

Kuan, W.K., Jin, G., Xin, P., Robinson, C., Gibbes, B. and Li, L. (2012), "Tidal Influence on Seawater Intrusion in unconfined Coastal Aquifers", Water Resources Research, 48:W02502.

Li, L., Barry, D. A. and Pattiaratchi, C.B. (1997), "Numerical Modeling of Tidal-Induced Beach Water Fluctuations", Coastal Engineering 30, pp. 105-123.

Li, L., Barry, D. A., Stagnitti, F., and Parlange, J.Y. (1999), "Tidal Along-Shore Groundwater Flow in a Coastal Aquifer", Environmental Modeling and Assessment 4, pp. 179-188.

Li, L., Barry, D.A., Stagnitti, F., Parlange, J.Y. and Jeng, D.S. (2000), "Beach Water Table Fluctuations Due to Spring-Neap Tides: Moving Boundary Effects", Adv. Water Resour. 23 (8), pp. 817–824.

Monachesi, L. B. and Guarracino, L., (2011). "Exact and Approximate Analytical Solutions of Groundwater Response to Tidal Fluctuations in a Theoretical Inhomogeneous Coastal Confined Aquifer", Hydrogeology Journal, 19, pp.1443-1449.

Nielsen, P. (1990), "Tidal Dynamics of the Water Table in Beaches", Water Resources Research 26 (9), pp. 2127–2134.

Philip, J.R. (1973), "Periodic Non-linear Diffusion: an Integral Relation and Its Physical Consequences", Aust. J. Phys. 26, pp. 513-519.

Smiles, D.E. and Stokes, A.N. (1976), "Periodic Solution of Nonlinear Diffusion Equation Used in Groundwater Flow Theory: Examination Using a Hele-Shaw Model", J. Hydrol. 31, pp. 27-35.

Strack, O. D. L. (1976), "A Single-Potential Solution for Regional Interface Problems in Coastal Aquifers", Water Resources Research, 12, pp. 1165-1174.

Taigbenu, A. E., Liggett, J.A. and Cheng A.H-D. (1984), "Boundary Integral Solution to Seawater Intrusion into Coastal Aquifers", Water Resource. Res.;20, pp. 1150–1158.

Todd, D. K. (1974), "Salt-water Intrusion and its Control", Water technology resources. Journal of American Water Works Association, 66(3), pp. 180-187.

Wang, J and Tsay,T. (2001), "Tidal Effect on Ground Water Motion", Transport in Porous Media,43, pp.159-178.

Yeh, H. D., Huang, C. S., Chang, Y. C. and Jeng D. S. (2010), "An analytical solution for tidal fluctuations in unconfined aquifers with a vertical beach",Water Resour. Res., 46, W10535, doi:10.1029/2009WR008746.